David Tomás Sánchez Martínez
Lourdes García Rodríguez
(coordinadores)

# Proceedings of the 7th International Seminar on ORC Power Systems

Editorial Universidad de Sevilla

Proceedings of the 7th International Seminar on

# ORC

# Power Systems

David Tomás Sánchez Martínez
Lourdes García Rodríguez
(coordinadores)

Proceedings of the 7th International Seminar on

# ORC Power Systems

# (ORC2023)

4th to 6th
SEPTEMBER
SEVILLE 2023

EDITORIAL UNIVERSIDAD DE SEVILLA

Sevilla, 2024

Colección Actas
Núm.: 91



Review chairs of the 7th International Seminar on ORC Power Systems

Prof. Christoph Wieland (University of Duisburg-Essen) - *Review Chair*
Prof. Sotirios Karellas (National Technical University of Athens) - *Review Co-Chair*
Prof. Teemu Turunen-Saaresti (LUT University) - *Review Co-Chair*
Dr. Diego-César Alarcón-Padilla (Plataforma Solar de Almería - CIEMAT) - *Review Co-Chair*
Dr. Francesco Crespi (Universidad de Sevilla) - *Review Co-Chair*



ISBN 978-84-472-2745-7
DOI: https://dx.doi.org/10.12795/9788447227457

Diseño de cubierta y maquetación: los autores

# INDEX OF CONTRIBUTIONS

DOI: https://dx.doi.org/10.12795/9788447227457_110


# NUMERICAL INVESTIGATION OF ORGANIC VAPOR FLOW EFFECTS ON A MICRO-SCALE RADIAL TURBOCOMPRESSOR

Andrés Sebastián*, Rubén Abbas, Manuel Valdés

*Universidad Politécnica de Madrid (UPM), José Gutiérrez Abascal 2, 28006 Madrid, Spain*
*Corresponding Author: andres.sebastian@upm.es

## ABSTRACT

Radial turbocompressor-based heat pump-like systems are currently being studied for novel environmentally friendly energy applications. Hence, the development of small centrifugal compressors using different organic vapors is in the spotlight. This work proposes some upgrades to a previously developed similarity-based and generalized flow turbomachinery scaling methodology for organic vapors. The main objective is to conduct a numerical study of the non-ideal effects on micro-scale radial turbocompressor working at different operating conditions using two organic fluids (propane and isobutene). Results show a good degree of agreement between the analytical predictions and the numerical simulation. Furthermore, the use of new similarity parameters is discussed in the range of the operating conditions of the study. The findings of this work set out that some intrinsic vapor effects are well predicted by the proposed methodology, which allows the micro-turbocompressors scaling from ideal gas to vapor flow conditions.

## 1 INTRODUCTION



Research and development of novel sustainable technologies is required to accomplish the necessary transition towards a low-carbon global energy model. There is a wide range of potential technologies such as increased-efficiency heat pumps (Schiffmann and Favrat, 2010), polygeneration systems (Sebastián *et al*., 2021a), or different proposals of thermal energy storage systems (Steger *et al.*, 2020), where the use of downsized radial turbocompressors might be proposed using working fluids other than air, such as organic vapors. Radial micro-turbocompressors, also referred to as micro centrifugal compressors, are classified according to Casey et al. (2013) for having impeller outer diameters less than 30 mm and rotational speeds greater than 200 kmin$^{-1}$. Due to the increased interest in turbomachinery for organic Rankine cycles, there has been intense research work during the last decades devoted to the analysis, design, experimentation and manufacturing of organic axial and radial-flow turbines (Macchi and Astolfi, 2017). Hence, there is ongoing research on the characterization of non-ideal compressible flows on turbines performance (Romei *et al* 2020, Baumgärtner *et al* 2021). Indeed, recent studies concerning the extension of the dimensional analysis for turbomachinery operating with dense vapor flows have been published, such as Giuffre and Pini (2021). However, according to aus der Wische and Reinker (2022), there are still gaps in the general comprehension of turbomachinery beyond typical perfect gas assumptions such as the dimensional analysis and performance laws using organic vapor flows.

Research efforts are required as a consequence of the rising trend of studying organic vapor compressions, instead of expansions, for further applications as those environmentally friendly energy systems. Indeed, the influence of the isentropic exponent on similarity conditions and proposed corrections on compressor performance indicators have been discussed by Van den Braembussche (2019) and Casey and Robinson (2021). In addition, novel similarity methods and corrections were proposed for different working media apart from organic vapors, such as supercritical conditions (Jeong *et al*., 2020) or noble gases (Zou and Ding, 2018). The theoretical framework for the analysis of one-dimensional flows of perfect gases is currently extended to the case of non-ideal compressible flows through different studies such as Tosto *et al*., (2021), where the molecular complexity and dense-vapor effects are analyzed in compressible internal flows. Giuffre *et al* (2022) conducted a numerical investigation on the effect of working fluid on high-speed centrifugal compressors and provided further evidence that efficient designs operating with organic may feature pressure ratios up to five at off-design, are feasible from the dynamic standpoint. All these efforts lead to the concept presented by aus der Wische and Reinker (2022) for generalized performance laws for organic vapor flow turbomachinery, being specifically tested for radial turbocompressors.

This work aims to conduct a numerical study based on computational fluid dynamics applied to a small-scale radial turbocompressor assessing its performance using air as well as two different organic fluids (isobutane and propane) at different operating points keeping dynamical similitude conditions. The novelty in this work lies in the assessment and improvement of the abovementioned generalized performance laws for organic vapors, evaluating its adequacy when using new similarity numbers better suited to turbocompressors operating in vapor conditions. The structure of the manuscript is as follows: after establishing the scope and the grounds of the paper in the introduction section, Section 2 presents the analytical and numerical methodology together with the operating points selection and the definition of the reference machine; Section 3 shows the obtained results and the numerical comparison among the selected set of working conditions. Finally, the main conclusions are drawn in Section 4.

## 2 METHODOLOGY

This section describes the methods and actions developed to carry out the numerical investigation proposed. First, a generalized dimensional analysis is set for organic vapor turbomachinery which will be used to generate operating points keeping dynamic similarity conditions, also named homologous points. Then, the numerical modelling approach is explained along with the definition of the micro-scale radial turbocompressor geometry. Finally, the selection of the working fluids and the operating points to be analytically and numerically studied is discussed.

### 2.1 Dimensional analysis for organic vapor turbomachinery



Generalized flow scaling laws are required when dealing with compressible flow turbomachinery using fluids other than air. As introduced in the previous section, aus der Wische and Reinker (2022) developed a novel formulation for the dimensional analysis of turbomachinery working with non-ideal fluids, which intends to be valid also for complex fluids (fluids with a behavior far from the ideal) such as organic vapors. This functional relationship based on Buckingham's Π-theorem goes beyond the conventional approach of perfect gas and is expressed in Equation 1. Total-to-total pressure ratio and efficiency are chosen as key performance indicators. Then, blade Mach number ($\Pi_n$), dimensionless mass flow rate ($\Pi_{\dot{m}}$) and Reynolds number (*Re*) are formulated as usually found in literature. Now, two new similarity dimensionless groups are raised. The first one is called modified Eckert number ($Ec^{*1/2}$), which can be replaced by γ-similarity in case of a perfect gas and should be understood as a representation of dissipation effects. Finally, another new similarity number is proposed, called the Traupel number (*Tr*), which takes into account the non-perfectness of the fluid through the partial derivative of the compressibility factor along an isentropic compression/expansion process instead of simply the compressibility factor (*Z*). For a perfect gas (or vapor), $Tr$=0 holds.

$$\frac{p_{02}}{p_{01}}, \eta = f\left(\frac{nD}{a_{01}}, \frac{\dot{m}\sqrt{RT_{01}}}{p_{01}D^2}, \frac{\rho n D^2}{\mu}, \frac{nD}{(RT_{01})^{1/2}}, \rho n^2 D^2 \frac{\partial Z}{\partial p}\bigg|_s\right) \tag{1}$$

On this innovative basis, some modifications are proposed for the sake of a major generalization following Sebastián *et al.* (2021b), as Equation 2 holds. First, inlet stagnation properties are set to all the fluid properties considered in the analysis. Then, the use of stagnation inlet speed of sound is proposed in the dimensionless mass flow rate in order to not consider any perfect gas assumption. Finally, isentropic stage loading or head coefficient ($\Delta h_s/a_{01}^2$) is proposed instead of the direct use of total-to-total pressure ratio. This may improve the characterization of the compression/expansion dynamical similarity preservation since isentropic enthalpy rise can be kept as a function of media speed of sound without any kind of perfect gas assumption. One may note that neither the ideal adiabatic specific heat ratio ($\gamma=c_p/c_v$) nor the real isentropic pressure-volume exponent ($\gamma_{pv}$), see Equation 3, are taken as independent dimensionless numbers.

$$\frac{\Delta h_{0s}}{a_{01}^2}, \eta = f\left(\frac{nD}{a_{01}}, \frac{\dot{m}}{\rho_{01}a_{01}D^2}, \frac{\rho_{01}nD^2}{\mu}, \frac{nD}{(RT_{01})^{1/2}}, \rho_{01}n^2D^2\frac{\partial Z}{\partial p}\bigg|_s\right) \tag{2}$$

$$\gamma_{pv} = -\frac{v}{p}\frac{\partial p}{\partial v}\bigg|_s = -\gamma\frac{v}{p}\frac{\partial p}{\partial v}\bigg|_T \tag{3}$$

Once the functional relationship is set, one must choose which dimensionless numbers are required to be kept to provide any other operating points when varying boundary conditions or working fluid. Through the two first dimensionless groups, the calculation of homologous rotational speed and mass flow rate is straightforward. The third group influence may be omitted if Reynolds number is large enough not to fall below the critical threshold under which viscous friction on the boundary layer becomes dominant. Finally, the modified Eckert and the Traupel numbers are selected as the degree of freedom of the system. Hence, their value will be analyzed and compared to seek the method's potential deviations. Considering that dynamical similarity is preserved, efficiency and dimensionless isentropic enthalpy rise must be kept. Total-to-total pressure ratio can be then analytically calculated through real gas data properties taken from REFPROP database.

The proposed analytical methodology will be used for a reference geometry of a small-scale turbocompressor to generate a set of operating points at different working conditions. This variation includes the change of working fluid from air to two organic vapors. Hence, the novel formulation presented above will generate the required boundary conditions for the numerical simulation, which will be then compared to the scaling laws to check the prevalence of dynamical similarity conditions.

### 2.2 Numerical modelling and reference turbocompressor

638

The numerical model used for this analysis is an upgraded version of the micro-scale radial compressor model developed in Sebastián *et al.* (2021b) using ANSYS-CFX. It is a one-stage air centrifugal compressor consisting of a 20 mm impeller with seven blades and seven splitter blades rotating at 220 $kmin^{-1}$ at design conditions and a vaneless diffuser. At the design point, the micro-compressor with air as working fluid provides an overall total-to-total pressure ratio around 1.4 consuming 330 W. Further technical data can be also found in Sebastián *et al.* (2023).

The stage modeled is formed by a seventh part of the straight inlet duct, the impeller and the vaneless diffuser passage of the reference micro-scale radial turbocompressor, providing a reference mesh of 4.8 million cells, with an average cell size of 0.043 mm. The Grid Convergence Index (GCI) proposed by Celik *et al* (2008) is obtained to determine the error band on the convergence solution (discretization error). Two additional meshes have been studied following the Celik's method: a coarse mesh (2.2 million cells, 0.055 mm average cell size) and a fine mesh (10.9 million cells, 0.032 mm average cell size). The GCI value from the fine grid to the intermediate ($GCI_{12}$) based on the total-to-total pressure ratio is 0.09%, well below 0.54% of the GCI from the intermediate to the coarse mesh ($GCI_{23}$). Hence, these very low values allow the use of the reference mesh for this numerical problem ensuring stable and grid-insensitive results. The inlet condition is specified in terms of the total temperature and pressure of the fluid; the outlet sets the mass flow rate. This inlet-outlet configuration is the one that provides the best numerical stability. The lateral faces of the fluid domain are defined as rotational periodic boundaries to simulate the full stage as Figure 1 shows. Stationary-rotating interfaces were solved by means of the mixing plane approach. Working fluid real properties are characterized using the Aungier-Redlich-Kwong model and $\kappa$–$\omega$ shear stress transport is the turbulence model selected. Regarding the solver control parameters, both high-resolution advection schemes and turbulence numerics have been applied. The convergence criterion of the root mean square residuals is set to $10^{-5}$ while ensuring convergence of total-to-total pressure ratio and polytropic efficiency.

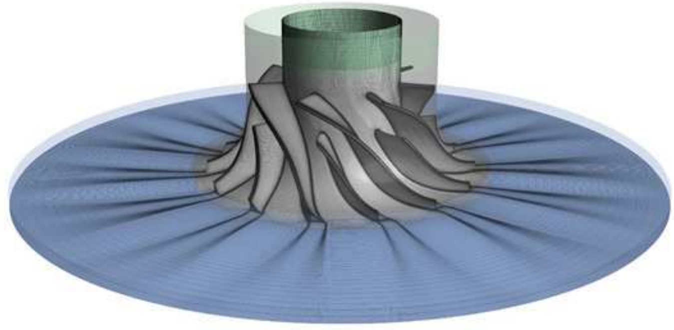

**Figure 1:** Meshed view of the numerical model solid parts (inlet, impeller and diffuser) of the reference micro-scale centrifugal compressor geometry.

As mentioned above, the design working fluid of the reference geometry is air at inlet design operating point conditions 1 bar and 20 ºC. At these conditions, the chord-based Reynolds number falls in the range of $10^4$-$10^5$, resulting in a viscous sublayer thickening where viscous effects increase. This may affect the velocity flow field and Reynolds number corrections must be used if dynamical similarity is sought. In order to provide a reference operating point at a turbulent enough flow regime, new reference conditions of inlet air at 5 bar and 20 ºC are established applying the methodology proposed by Sebastián *et al.* (2021b), which is analytically and numerically validated. Hence, these conditions are the reference for keeping dynamical similarity through the method proposed in previous Equation 2. This allows to generate homologous operating points using organic vapor at any conditions, obtaining the new rotational speed, mass flow rate and inlet pressure/temperature, which are used as inputs for the numerical simulations. The next section will deal with the selection of the boundary conditions of these new sets using organic fluids.



### 2.3 Organic vapors and operating points selection

Two low global warming potential and zero ozone depletion potential non-toxic organic compounds have been selected for this analysis: propane and isobutane. These working fluids have been proposed for different environmentally-friendly small-scale turbo-heat-pump-based energy systems, such as Sebastián *et al.* (2021a). Figure 2 collects in an enthalpy-entropy diagram the selected operating points for both propane and isobutane working fluids, where also temperature contour levels can be observed. A set of homologous points are calculated at 1 bar and 25 ºC inlet conditions for both media. These corresponding polytropic compression lines are represented far from the saturation line at increased specific entropy values, but still in the vapor region. Then, three operating points are fixed in the pursuit of simulating a near-saturation line compression, similar to those compressions for heat pump-like systems. Inlet pressure has been selected in relation to the saturation pressure at 5 ºC, 25 ºC and 45 ºC considering a compressor suction superheat control of 5 K. These boundary condition temperature levels have been selected to represent evaporating lines for heat pumps providing cooling, air heating and heat upgrading, respectively. These eight homologous operating points will be the object of numerical analysis in the next Section.

These dense vapor compression processes entail a non-perfect thermodynamic behavior. Figure 3a shows the compressibility factor evolution at isentropic compressions lines for the studied compressors operating points. While the perfect gas behavior can be noted using air, propane and isobutane operating points provide significant variation of $Z \neq f(s)$. This means that the selected conditions are closer to a non-perfect gas than to a perfect vapor behavior. Meanwhile, Figure 3b represents the variation in the speed of sound at the selected compression lines where its decrease along the compression features non-ideal effects. These operating points, Pr. #2-4 and Ib. #2-4, feature a fundamental derivative $\Gamma$ below 1 (in the range of 0.88-0.98). One may also note a lower variation using the organic vapors than using air, which may ease the dynamical similitude behavior preservation.

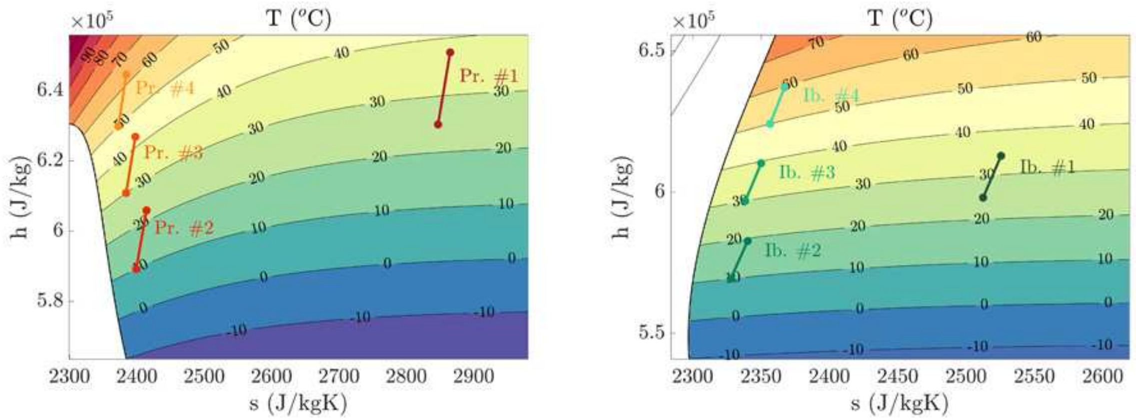


a) Propane b) Isobutane

**Figure 2:** Temperature contours on an enthalpy-entropy diagram for both organic fluids. The resultant compression lines for the set of studied operating points are marked and labelled. Pr. and Ib. stands for propane and isobutene, respectively.

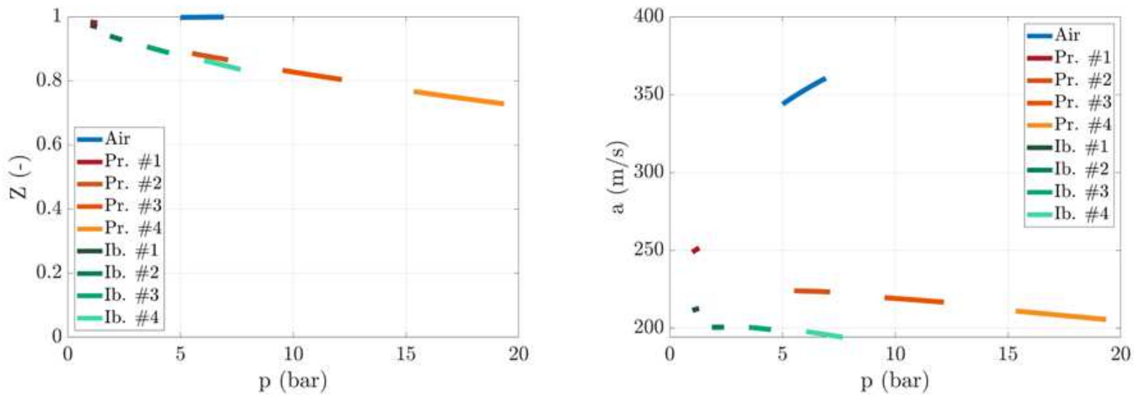


a) b)

**Figure 3:** Compressibility factor (a) and speed of sound (b) evolution at the studied isentropic compression lines for the set of new operating points to be numerically simulated.

## 3 RESULTS

The results section is structured as follows: first, the analytical results obtained through the proposed generalized similarity-based methodology for the selected organic fluids and operating conditions set in the previous section; next, numerical results are shown to confirm dynamical similarity preservation; finally, averaged numerical key indicators are compared with analytical indicators to understand the source of deviations when scaling to organic fluids.

### 3.1 Analytically-obtained similitude for the selected organic operating points

Table 1 collects the results of applying the similarity-based methodology to the set of points selected for this analysis. One may note that keeping dynamical similitude while varying the working fluids and pressure/temperature conditions leads to a blade Mach number ($\Pi_n$), a dimensionless mass flow rate ($\Pi_{\dot{m}}$) and the isentropic stage loading coefficient ($\Delta h_s/a_{01}^2$) constant. *Re* values are all above $10^5$ which allows neglecting the influence of this number on key performance indicators assuming a fully developed turbulent flow regime. Regarding $Ec^{*0.5}$, small deviations are observed for both propane and isobutene. These deviations increase following the rise in compressor inlet pressure, leading to an $Ec^{*0.5}$ study range of 0.183-0.253. Meanwhile, near-zero *Tr* values are obtained with negative values due to the negative compressibility factor slope along the previously shown organic compressions. It is interesting to highlight that despite these notable slopes shown in previous Figure 3a, the factor composed of rotational speed, density and characteristic dimensions is not large enough to obtain a non-zero *Tr*. For instance, the first factor of *Tr* in Pr. #3 operating point is $4.4 \cdot 10^4$, while its compressibility factor slope is $-1.1 \cdot 10^{-7}$. A doubled rotational speed and five times the inlet density would be needed to obtain a *Tr* around -0.1. This means that at present subsonic Mach conditions (<0.6) using the proposed organic vapors, non-ideal flow can be assumed as perfect vapor behavior. Finally, resultant variations of the total-to-total pressure ratio ($\beta_{TT}$) are shown.

**Table 1:** Resultant dimensionless numbers calculated using the proposed scaling laws for the selected operating points. Pr. and Ib. stands for propane and isobutene, respectively.

| | Air (ref) | Pr. #1 | Pr. #2 | Pr. #3 | Pr. #4 | Ib. #1 | Ib. #2 | Ib. #3 | Ib. #4 |
|---|---|---|---|---|---|---|---|---|---|
| $p_{01}$ (bar) | 1.0 | 1.0 | 5.5 | 9.5 | 15.3 | 1.0 | 1.9 | 3.5 | 6.0 |
| $T_{01}$ (ºC) | 20 | 25 | 10 | 30 | 50 | 25 | 10 | 30 | 50 |
| $\Pi_n$ (-) | 0.214 | | | | | | | | |
| $\Pi_{\dot{m}}$ (-) | 0.043 | | | | | | | | |
| $Re$ (-) | $4.8\ 10^5$ | $2.4\ 10^5$ | $1.4\ 10^6$ | $2.2\ 10^6$ | $3.2\ 10^6$ | $2.9\ 10^5$ | $5.9\ 10^5$ | $1.0\ 10^6$ | $1.6\ 10^6$ |
| $Ec^{*1/2}$ (-) | 0.253 | 0.222 | 0.207 | 0.196 | 0.183 | 0.217 | 0.213 | 0.206 | 0.196 |
| $Tr$ (-) | 0 | -0.001 | -0.003 | -0.005 | -0.006 | -0.001 | -0.002 | -0.003 | -0.005 |
| $\Delta h_s/a_{01}^2$ (-) | 0.242 | | | | | | | | |
| $\beta_{TT}$ (-) | 1.384 | 1.306 | 1.290 | 1.277 | 1.261 | 1.294 | 1.289 | 1.280 | 1.268 |

### 3.2 Numerical validation of velocity flow field similarity

This subsection aims to prove and validate that dynamical similarity is achieved in numerical simulations through the inputs generated by the proposed generalized scaling laws. Mass flow averaged absolute (*Ma*) and relative ($Ma_w$) Mach numbers are shown in Figure 4a at different stations along the compressor stage. Reference air design point is plotted together with the eight selected operating conditions using propane and isobutane. Their relative differences with the reference case are shown in Figure 4b. One may note that an average ±2.5% of discrepancy is found. In addition, there is a reasonably good Mach agreement among the operating points using organic vapor flows, especially across the impeller. This confirms that homologous conditions provided by the analytical scaling entails that dynamical similarity conserves the dominant flow Mach numbers.



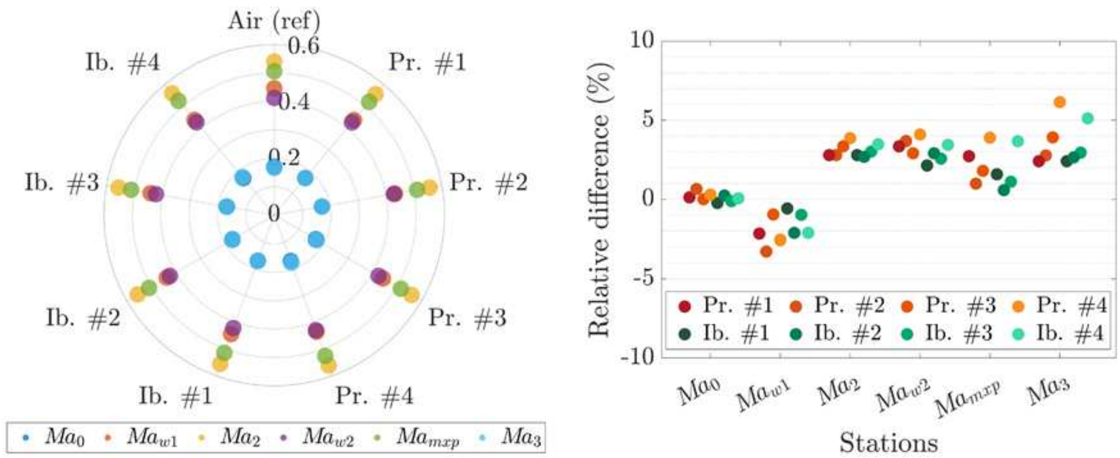


a) b)

**Figure 4:** Absolute (*Ma*) and relative ($Ma_w$) mass flow averaged Mach number at different stations: a) values and b) relative difference vs air. (0: inlet, 1: near impeller leading edge, 2: near impeller leading edge, *mxp*: mixing plane, 3: diffuser outlet) for all the operating points set selected.

Two organic operating points using propane at the highest pressure (Pr. #4) and isobutane at the lowest (#Ib. 1) are selected to verify that not only averaged Mach numbers are preserved but also the velocity flow fields. Figures 5a and 5b show both absolute and relative Mach number contours on a compressor blade-to-blade view at half span location to perform a qualitative comparison One may observe the similar main flow structure, the similar incidence at leading edge, and the same tip-leakage-induced bubble at the trailing edge suction side. Therefore, it can be confirmed that homologous working conditions on an organic micro-scale turbocompressor are achieved.

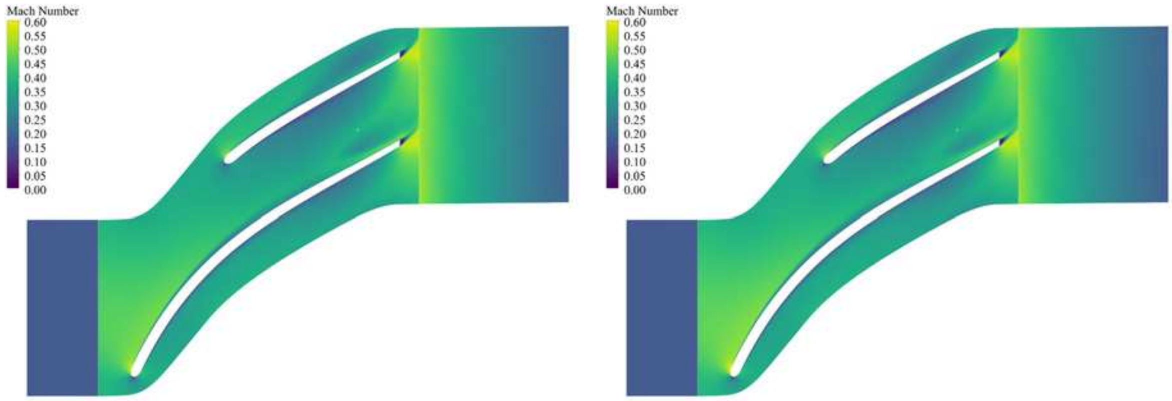


a) Pr. #4 b) Ib. #1

**Figure 5:** Mid-span blade-to-blade view of stationary and relative Mach number for two selected operating points at organic vapor conditions.

### 3.3 Numerical-analytical comparison

Once similitude is numerically proven for the selected organic vapors conditions, it is interesting to analyze the analytical-numerical deviations on key performance indicators and the emerging trends between different thermodynamic properties. It is shown the relationship between the total-to-total pressure ratio and the compressibility factor (Figure 6a) and also between the real isentropic pressure-volume exponent (Figure 6b) through the proposed analytical dynamic similitude method (DS) and using the numerical model (CFD) for all the simulated operating points. One may remark that pressure ratio trend is properly predicted despite $Z$ and $\gamma_{pv}$ are not explicitly considered as independent dimensionless groups scaling the organic fluid through the DS method. The relationship between the isentropic loading coefficient and the mentioned thermodynamic properties can be shown in Figure 6d-6e. Deviations between analytical and numerical results do not form an identifiable pattern as expressed in the mentioned plots. This means that the key performance indicator is not exactly kept and its deviations could not be followed by $Z$ and $\gamma_{pv}$, which are two of the main non-ideal gas thermophysical properties. In other words, isentropic loading coefficient deviations are not caused by the organic vapor non-perfectness itself since good matches can be found at high and low $\gamma_{pv}$.

As explained in Subsection 3.1, variations on Traupel number cannot be responsible for these variations since their values were in the range -0.006 up to 0 in the selected conditions set. Hence, alterations on the second new dimensionless number (the modified Eckert number) are studied. Figure 6c shows the impact of these variations on the relative static impeller outlet temperature. A substantial change when moving to organic vapors can be appreciated and then is kept among the different data points. Nevertheless, Figure 6f does not show a clear pattern between both parameters. Hence, it cannot be stated that the variations on this new dimensionless number in the range of 0.183-0.253 convey an effect on the chosen similitude key performance indicator. Overall, one may find a notable good agreement between CFD and DS method on the resultant total-to-total pressure ratio, thus the scaling analysis works.

642

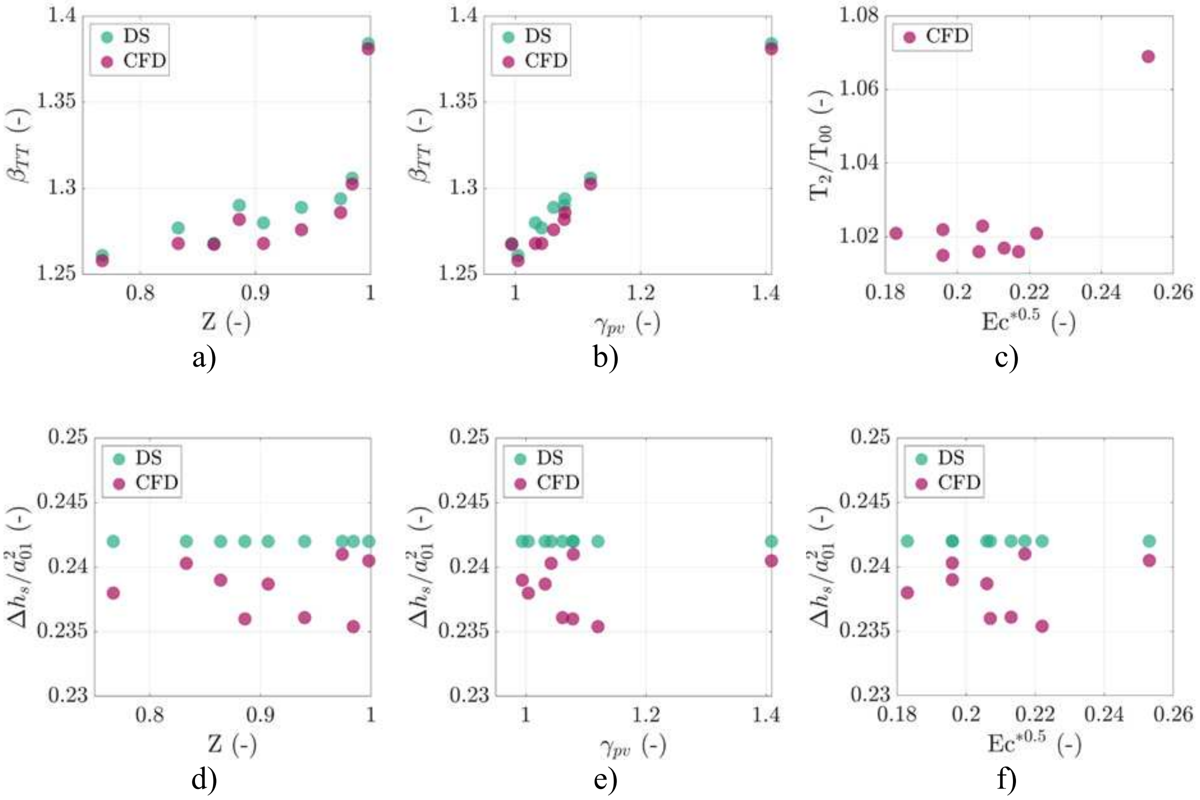


**Figure 6:** Scatter plots among selected variables for the whole set of operating points comparing dynamical similitude (DS) calculations versus numerically obtained (CFD) results.

643

## 4 CONCLUSIONS

The present study investigates the non-ideal effects on a small radial turbocompressor when similitude is sought for two organic fluids at different operating conditions near the saturation line, where heat pump-like systems work. In light of the results of this paper, the following findings can be drawn:

- The upgraded version of the generalized flow turbomachinery dynamic similarity method proposed in this work is able to capture non-ideal effects and provides an accurate pressure ratio prediction including implicit variations on compressibility factor and real isentropic pressure-volume exponent. These trends have been numerically validated. Hence, the scaling analysis can be performed without taking compressibility factor and real isentropic pressure-volume exponent as independent dimensionless groups.
- Dynamical similarity conditions are numerically checked through averaged Mach numbers across the stage but also along the velocity flow fields. This means that analytically-generated input conditions to the CFD model are well computed.
- The set of operating points at different conditions and organic vapors (propane and isobutane) working with the reference micro-scale turbocompressor provide Traupel number values close to zero. Therefore, perfect vapor behavior is expected as Traupel number does not imply a substantial effect. Regarding the modified Eckert number, small variations are detected without a clear trend related to the isentropic loading coefficient.
- Radial micro-turbocompressors scaling from ideal gas to perfect vapor conditions is allowed under the conditions of this study for the pressure ratio prediction.

This study has confirmed the suitability of the scaling method for high-speed radial micro-turbocompressor operating in a thermodynamic area where heat-pump-like systems usually work when using propane and isobutane. Despite the high rotational speed, the near-zero Traupel number leads one to assume perfect vapor behavior. One may wonder when these assumptions cannot be extended. On this basis, the next step will be to study micro-compressors providing higher pressure ratios per stage, to fulfil more closely the requirements of heat pump-based applications. Furthermore, the notable focus on high-temperature heat pumps makes it also interesting to study scaling methods when more relevant non-ideal flow effects dominate.

## REFERENCES


aus der Wiesche, S. and Reinker, F., 2022, Dimensional analysis and performance laws for organic vapor flow turbomachinery, Energy, 257, 124635.

Baumgärtner, D., Otter, J. J. and Wheeler, A. P. S., The effect of compressibility factor on turbine performance, Proceedings of the ASME Turbo Expo 2021: Turbomachinery Technical Conference and Exposition, Volume 4, V004T06A020.

Casey, M., Krähenbuhl, D., Zwyssig, C., 2013, The Design of Ultra-High-Speed Miniature Centrifugal Compressors, Proceedings of 10th European Conference on Turbomachinery Fluid dynamics & Thermodynamics, ETC10-004, Lappeenranta, Finland.

Casey, M. and Robinson, C., 2021, Radial Flow Turbocompressors, Cambridge University Press.

Celik, I. B., Ghia, U., Roache, P. J., Freitas, C. J., Coleman, H., and Raad, P. E., 2008, Procedure for estimation and reporting of uncertainty due to discretization in CFD applications. Journal of fluids Engineering-Transactions of the ASME, 130(7):078001–078001–4.

Giuffre, A. and Pini, M., 2021, Design guidelines for axial turbines operating with non-ideal compressible flows, Journal of Engineering for Gas Turbines and Power 143.1: 011004.

Giuffre, A., Colonna, P. and Pini, M., 2022, The effect of size and working fluid on the multi-objective design of high-speed centrifugal compressors, International Journal of Refrigeration, 143, 43-56.

Jeong, Y., Son, S., Cho, S. K., Baik, S., Lee, J. I., 2020, Evaluation of supercritical CO2 compressor off-design performance prediction methods, Energy, 213, 119071.

Macchi, E. and Astolfi, M., 2017, Organic Rankine Cycle (ORC) Power Systems, Woodhead Publishing Series in Energy, Elsevier.

Romei, A., Vimercati, D., Persico, G. and Guardone, A., 2020, Non-ideal compressible flows in supersonic turbine cascades, Journal of Fluid Mechanics, 882, A12.

Schiffmann, J. and Favrat, D., 2010, Design, experimental investigation and multi-objective optimization of a small-scale radial compressor for heat pump applications, Energy, 35, 436–450.

Sebastián, A., Abbas, R., Valdés, M., Rovira, A., 2021, Modular micro-trigeneration system for a novel rotatory solar Fresnel collector: A design space analysis, Energy Conversion and Management, 227, 113599.

Sebastián, A., Abbas, R., Valdés, M., 2021, Analytical prediction of Reynolds-number effects on miniaturized centrifugal compressors under off-design conditions, Energy, 227, 120477.

Sebastián, A., Abbas, R., Valdés, M., 2023, Experimental investigation of key aerothermal phenomena in micro-scale radial turbocompressors, Thermal Science and Engineering Progress, 39, 101748.

Steger, D., Regensburger, C., Eppinger, B., Will, S., Karl, J., Schlucker, E., 2020, Design aspects of a reversible heat pump - organic rankine cycle pilot plant for energy storage. Energy, 208, 118216.

Tosto, F., Lettieri, C., Pini, M., Colonna, P., 2021, Dense-vapor effects in compressible internal flows, Phys. Fluids, 33, 086110.

Van den Braembussche, R., 2019, Design and analysis of centrifugal compressors, JohnWiley&Sons.

Zou, Z. and Ding, C., 2018, A new similarity method for turbomachinery with different working media, Applied Thermal Engineering, 133, 170–178.




## ACKNOWLEDGEMENT

This research has been supported by the Spanish *Ministerio de Ciencia e Innovación* under the project of reference number PID2019-110283RB-C32. The authors also would like to thank the reviewers for their valuable feedback and insightful comments.

This book contains the compilation of works contributed to the *7th International Seminar on Organic Rankine Cycle Power Systems* (ORC 2023), held in Seville between the 4th and 6th of September 2023. The event was hosted by Universidad de Sevilla on behalf of the Knowledge Centre on Organic Rankine Cycle Technology (KCORC), incorporated in The Netherlands.

The ORC conference, organized biennially, stems as the only conference that is specific to ORC technology, therefore gathering a diverse community whose affiliation spans across all the interested stakeholders, not only in this particular technology but also and in a broader context, in the energy transition. Original equipment manufacturers, professional associations, end-users, investors, policy makers, academics, scientists feel at home at ORC 2023.

The almost 100 proceedings in this book cover a wide variety of topics, from fundamentals to system integration through component design, accounting for thermodynamic performance as well as component design. In addition to this, and as a new track in 2023, works on heat pump technology were also accepted in order to raise awareness of the strong ties between both technologies, specifically in energy storage applications.

This book provides an excellent overview of the current maturity of power systems based on Organic Rankine Cycle technology for applications as diverse as geothermal and waste heat recovery in industry or downstream of other prime movers (e.g., marine applications). It is also an excellent source of information to understand the current challenges faced by the technology, stemming from a very competitive market and increasingly stringent environmental regulations.

The organizers of ORC 2023 hope that the reader finds this work as exciting as the attendees to the conference and, maybe, make the decision to join the 8th edition to the conference in 2025.

KCORC
KNOWLEDGE CENTER
ORGANIC RANKINE CYCLE

eus EDITORIAL
UNIVERSIDAD DE SEVILLA